ELSEVIER

Biophysical Chemistry 93 (2001) 141–157

Biophysical Chemistry

www.elsevier.com/locate/bpc

# Comparative investigations of biopolymer hydration by physicochemical and modeling techniques

Helmut Durchschlag[a,*], Peter Zipper[b]

[a] *Institute of Biophysics and Physical Biochemistry, University of Regensburg, Universitätsstrasse 31, D-93040 Regensburg, Germany*

[b] *Physical Chemistry, Institute of Chemistry, University of Graz, Heinrichstrasse 28, A-8010 Graz, Austria*

Received 5 April 2001; received in revised form 21 June 2001; accepted 21 June 2001

**Abstract**

The comparative investigation of biopolymer hydration by physicochemical techniques, particularly by small-angle X-ray scattering, has shown that the values obtained differ over a wide range, depending on the nature of the polymer and the environmental conditions. In the case of simple proteins, a large number of available data allow the derivation of a realistic average value for the hydration (0.35 g of water per gram of protein). As long as the average properties of proteins are considered, the use of such a default value is sufficient. Modeling approaches may be used advantageously, in order to differentiate between different assumptions and hydration contributions, and to correctly predict hydrodynamic properties of biopolymers on the basis of their three-dimensional structure. Problems of major concern are the positioning and the properties of the water molecules on the biopolymer surface. In this context, different approaches for calculating the molecular volume and surface of biopolymers have been applied, in addition to the development of appropriate hydration algorithms. 

*Keywords:* Biopolymer hydration; Catalase; Computer simulation; Hydrodynamic modeling; Parameter prediction; X-Ray data

## 1. Introduction

Hydration and solvent interactions in solutions of biological molecules are highly important phenomena responsible for the stabilization, structure, and function of biological molecules [1–19]. Although in the past, various physicochemical techniques have been applied to determine the hydration/solvation of biopolymers (e.g. [5,20–26]), the extent of water/solvent association, the properties of water/solvent molecules bound to biopolymers (e.g. volume and density of water molecules), and their localization on the macromolecule surface are still enigmatic, partly due to the fact that different approaches seem to yield quite different results. For precise determinations of the water content of biopolymers, some

* Corresponding author. Tel.: +49-941-943-3041; fax: +49-941-943-2813.

*E-mail address:* helmut.durchschlag@biologie.uni-regensburg.de (H. Durchschlag).

0301-4622/01/$ - see front matter 
PII: S0301-4622(01)00217-4

of the assumptions underlying the evaluation and interpretation of different techniques (e.g. concerning mass density and electron density of constituents, existence of water shells) seem to be inadequate. Therefore, comparative investigations of biopolymer hydration/solvation are a necessary prerequisite for understanding the behavior of biological matter. In addition, the application of several techniques of structural analysis requires qualified assumptions regarding hydration and/or buoyancy (e.g. for the prediction of hydrodynamic parameters from three-dimensional (3D) information [27–35]). While, nowadays, the experimental or theoretical determination of specific volumes poses no serious obstacle [36–39], the hydration/solvation problem is still the major limitation to many applications.

The goal of the present study was: (i) the investigation of hydration contributions of many classes of biopolymers, particularly of proteins, to establish the basis for more accurate possibilities to visualize water molecules on the polymer surface; and (ii) the use of the 3D structure of proteins together with scattering and hydrodynamic modeling approaches to test the assumptions concerning number and localization of water molecules bound to the protein surface. For the latter purpose, the calculation of solution scattering functions was used as an additional tool.

## 2. Molecules and methods

To obtain a survey of experimental data concerning volume, $V$, surface area, $S$, partial specific volume, $\bar{v}$, hydration, $\delta_1$, of various classes of biopolymers, literature values were examined. The data were selected from a large number of publications, and therefore, show quality differences in the data cited, obviously due to quite different accuracies achieved by different methods and authors. Concerning $V$ and $S$, data from small-angle X-ray scattering (SAXS) were preferred [40,41]. Hydration values were extracted from a variety of papers reliant upon quite different techniques for their estimation: e.g. isopiestic, calorimetric and densimetric experiments, hydrodynamic measurements including analytical ultracentrifugation (AUC), IR, Raman and NMR spectroscopy, SAXS, modeling techniques, etc. (e.g. [3,5,23]).

To illustrate a typical example in more detail, the tetrameric enzyme bovine catalase was chosen, the native enzyme containing one additional heme b and one $NADPH_2$ per subunit. Catalase has been analyzed by a variety of physicochemical techniques, including X-ray crystallography [42] and solution techniques such as SAXS [43,44], AUC and viscometry [45–47]. In order to correlate structural (X-ray) and hydrodynamic data, it has also been the subject of whole-body and multi-body modeling approaches [32,35,40,41,44,48,49].

In the following, only the parameters and methods pertinent to this study are mentioned in more detail.

Specific volumes can be determined experimentally, preferably by use of density measurements [36,39]. Experiments in multi-component solutions may be performed at constant molality or constant chemical potential of added solvent components. Partial and isopotential specific volumes ($\bar{v}$ and $v'$) or the isomolal and isopotential mass density increments, $(\partial\rho/\partial c)_m$ and $(\partial\rho/\partial c)_\mu$, may be used for the calculation of interaction parameters including information on the preferential binding/exclusion of water (hydration) and co-solvents [9,15,19,50].

The calculation of partial molar and partial specific volumes, $\overline{V}$ and $\bar{v}$, of low-molecular-weight and macromolecular organic compounds of non-ionic and ionic nature can be performed by means of a simple ab initio approach [37,38]. The calculated volumes are valid for aqueous solutions at 298 K (two-component solutions). The applied volume increments already take into account any interactions with the solvent water or other effects (ionization, hydration, ring formation, etc.) leading to volume changes (electrostriction) of different extents.

The analysis of SAXS curves, $I(h)$, and their Fourier transforms, the pair–distance distribution functions, $p(r)$, allows the determination of a variety of molecular parameters including radius of gyration, $R_G$, hydrated particle volume, $V$, and

surface area, $S$ [51,52]. $V$ can be obtained either directly from the second moment of $I(h)$ (Porod's invariant) or indirectly from a model derived from SAXS data. Accordingly, hydration values, $\delta_1$, may be obtained from a comparison of $V$ with the anhydrous volume, $V_{dry}$, calculated from molar mass, $M$, and $\bar{v}$ of the biopolymer:

$$\delta_1 = \left( \frac{VN_A}{10^{24}M\bar{v}} - 1 \right) \cdot \bar{v}\rho \quad (1)$$

where $\delta_1$ is given in g $g^{-1}$, $V$ in $nm^3$, $M$ in kg $mol^{-1}$, $\bar{v}$ in $cm^3$ $g^{-1}$, and the solvent density $\rho$ in g $cm^{-3}$; $N_A$ symbolizes Avogadro's number.

Sedimentation coefficients, $s$, are usually determined by AUC, diffusion coefficients, $D$, by AUC or dynamic light scattering, and intrinsic viscosities, $[\eta]$, from different types of viscometric measurements. The hydrodynamic parameters may be used to derive hydration values, $\delta_1$ [5,53,54].

The hydration of proteins may be calculated according to Kuntz [55]. His published data indicate a significant temperature dependence for the amount of water associated with the charged residues, and a strong pH effect for Glu, Asp and Tyr residues. The most obvious deficit of this approach is the assumption that each amino acid is exposed to the solvent; any correction for buried residues should increase with the size of the protein under consideration. However, according to Kuntz [55], the effects of buried residues (approx. $-10\%$ hydration in the case of lysozyme) and aggregation of subunits are considered to be of subordinate importance, and they should not generate major changes in hydration.

For the application of hydrodynamic and scattering modeling approaches, consideration of the appropriate amount of hydration is crucial [27–35,40,41,48,49,53,56–61]. Vice versa, modeling may be used to check the validity of $\delta_1$-values used, on the one hand, and the localization of water molecules on a biopolymer surface on the other.

In particular, multi-body approaches may be used efficaciously for the prediction of hydrodynamic properties from the atomic coordinates [35]. Using bead-modeling approaches and consideration of appropriate hydration contributions, hydrodynamic parameters such as sedimentation and diffusion coefficients as well as intrinsic viscosities may be estimated. The prediction of solution scattering data requires application of 'filling models' [35,41] instead of shell models [35,60], since the whole particle contributes to scattering. When applying this approach, various sophisticated procedures may be involved, e.g. efficient data reduction [31], bead modeling by overlapping spheres, consideration of hydration. Hydrodynamic calculations may be performed using García de la Torre's public-domain programs HYDRO [62] or HYDROPRO [35] or modifications thereof, since they enable the calculation of hydrodynamic quantities even by use of personal computers. Problems in the context of overlapping unequal spheres may be overcome by use of an ad hoc expression for the interaction tensor [31,32,63,64]. The crucial problem of hydration contributions may be solved by introduction of transformation factors acting on bead radii and/or bead coordinates, producing a uniform or non-uniform molecule expansion [27–34].

As an alternative approach to representing hydration, we modeled individual water molecules on the protein surface instead of 'blowing up' the whole molecule [27,28,30–34] or building a uniform water shell around the molecule [29], as was done in previous calculations. This was achieved by calculating the protein surface by use of surface calculation strategies, starting from the atomic coordinates, and positioning water molecules on the protein surface. The atomic coordinates of the protein were obtained from the Protein Data Bank [65] (accession code for beef liver catalase: 8CAT).

'Solvent-accessible surfaces' were originally defined and computed by Lee and Richards [66] by tracing out the surface accessible to the center of a probe sphere representing a solvent molecule as it rolls over the protein; this represents a kind of expanded 'van der Waals surface'. Refinements were achieved by Richards [67–69] introducing further surface definitions and strategies: the 'molecular surface' is formed by the 'contact sur-

face' and 're-entrant surface'.[1] More recent methods calculate analytically a smooth 3D contour about a molecule. Connolly's program MSRoll [70–72] computes a piecewise quartic molecular surface envelope surrounding the molecule. It yields contact, re-entrant, molecular and accessible areas and solvent-excluded volume of the entire molecule and of each interior cavity; and in addition to a 'dot surface', the program also computes a polyhedral surface of the molecule. Similarly, the program SIMS by Vorobjev and Hermans [73] produces a smooth invariant molecular dot surface, generating the smooth molecular surface by rolling two probe spheres; the method produces a quasi-uniform dot distribution on the molecular surface, which is invariant to molecular rotation and stable under changes in the molecular conformation. The main difference between the two programs seems to be the difference in homogeneity of the dot distribution.

Atomic coordinates were converted to hydrodynamic or SAXS models by representing each amino acid residue by a sphere (bead) of appropriate radius. The total volume of chosen spheres corresponded to the molecular volume of the anhydrous particle [33,74]. For hydrodynamic modeling, only the size (volume) of the beads was important, whereas for SAXS models, the beads were weighted according to their number of excess electrons [75].[2]

The resultant models were then hydrated as described in the following. We used the programs MSRoll and SIMS, the latter in adapted form, for computing a large number of dot surface points and normal vectors (approx. 50 000–100 000 in the case of catalase). The coordinates and normal vectors of the points, calculated on the basis of a probe radius of 0.14 nm, were used to construct potential positions of water molecules on the protein surface. A 'hydration algorithm' was then applied to select appropriate positions for placing individual water molecules on the protein surface. The number of water molecules assigned to each accessible amino acid residue was primarily based on the values given by Kuntz [55], assuming a minimum distance of 0.28 nm between water molecules. For modeling different degrees of hydration, the Kuntz values were uniformly increased by a factor $> 1$ [76]. Each selected water molecule was represented by a sphere of volume 0.0245 $nm^3$ [18,77,78], 0.0269 $nm^3$ [26,79] or 0.0284 $nm^3$, corresponding to volume decreases of approximately 20, 10, and 5% if compared to the volume of 0.0299 $nm^3$ [77] for bulk water.[3] In an alternative approach, the calculated volume of the water molecules adjacent to the amino acid residues on the surface was added to the amino acid volumes. A further alternative procedure expanded the volume of all (accessible and buried) amino acids according to the hydration values given by Kuntz [55], irrespective of whether they are buried inside or are located on the protein surface.

For hydrodynamic modeling, these hydrated models had to be reduced to a proper number of beads by means of the cubic grid approach [27,30,31]. SAXS curves, $I(h)$, of unreduced and reduced models were calculated by Debye's formula and converted to distance distribution functions, $p(r)$, by Fourier transformation [51,52]. The radii of gyration of the models were derived using the size and the coordinates of the beads ($R_{G,Hydro}$) or size, coordinates, and excess electrons ($R_{G,SAXS}$).

## 3. Determination of biopolymer volume and hydration

### 3.1. Physicochemical methods

For many applications, including AUC, solution

[1] The contact surface is the part of the van der Waals surface that can be touched by a water-sized probe sphere, the re-entrant surface is defined by the interior-facing part of the probe when it is simultaneously in contact with more than one atom [69].

[2] The number of excess electrons of a bead corresponds to the product of the bead volume and the electron density difference between the amino acid residue (represented by the bead) and the bulk water.

[3] As established by the cited X-ray, neutron and density investigations, the average density of bound water is approximately 10–20% larger than that of bulk water.

Table 1
Specific volumes and hydration of selected biopolymers, as revealed by different physicochemical techniques or calculative procedures by several authors.

| Molecule | Solvent conditions | Specific volume[a] | | Hydration[b] | | |
|---|---|---|---|---|---|---|
| | | $\bar{v}$ ($cm^3\ g^{-1}$) | Reference[d] | $\delta_1$ ($g\ g^{-1}$) | Method[c] | Reference[d] |
| *1. Simple Proteins:* | | | | | | |
| Albumin (bovine serum) | | | | | | |
| | | | | 0.15–1.07 | Different | [2] |
| | | | | 0.32 | Different (avg.) | [2] |
| | | | | 0.32 | SAXS | [23] |
| | | | | 0.32 | Isopiestic | [3] |
| | | | | 0.32–0.49 | Calorimetric | [3] |
| | | | | 0.33–0.52 | Hydrodynamic | [3] |
| | | | | 0.35 | Hydrodynamic | [5] |
| | | | | 0.36 | Dialysis | [84] |
| | | | | 0.40 | NMR | [3,55] |
| | | 0.735 | [40] | 0.55 | SAXS | [40] |
| | | | | 0.23 | Calc. | [15] |
| | | | | 0.36 | Calc. | [84] |
| | | | | 0.45 | Calc. | [3,55] |
| | 1 M NaCl | 0.735 | [85] | 0.23 | Thermodynamic | [15,85] |
| | 1 M NaCl | | | 0.24 | Thermodynamic | [9,19] |
| | 4 M GdmCl | 0.728 | [85] | 0.18 | Thermodynamic | [15,85] |
| | urea | | | 0.44 | NMR | [3,55] |
| | urea | | | 0.45 | Calc. | [3,55] |
| | pH 3 | | | 0.30 | NMR | [3,55] |
| | pH 3 | | | 0.32 | Calc. | [3,55] |
| | pH 4 | | | 0.32 | Calc.[e] | This study |
| | pH 6–8 | | | 0.45 | Calc.[e] | This study |
| | pH 10–12 | | | 0.47 | Calc.[e] | This study |
| Denatured | | | | 0.33 | Calorimetric | [3] |
| Catalase (bovine liver) | | | | | | |
| | | | | 0.29 | SAXS | [23] |
| | | 0.730 | [40] | 0.34 | SAXS | [41] |
| | | | | 0.70 | Diffusion | [2] |
| | | | | 0.40 | Calc.[e] | This study |
| | | | | 0.39 | Calc.[e,f] | This study |
| Citrate synthase (pig heart) | | 0.740 | [40] | 0.33 | SAXS | [40] |
| | | | | 0.39 | Calc.[e] | This study |
| | + oxaloacetate | 0.739 | [40] | 0.27 | SAXS | [40] |
| Lysozyme (chicken egg white) | | | | $0.19 \pm 0.10$ | SAXS-modeling | [86] |
| | | | | 0.23–0.89 | Different | [2] |
| | | | | 0.25 | Isopiestic | [3] |
| | | | | 0.29 | Different (avg.) | [2] |
| | | | | 0.3 | Calorimetric | [3] |
| | | | | 0.31–0.34 | Different | [11] |
| | | 0.702 | [40] | 0.32 | SAXS | [23,40] |
| | | | | 0.34 | NMR | [3,55] |
| | | | | 0.34–0.52 | Hydrodynamic | [3] |
| | | | | 0.55 | Dialysis | [84] |

Table 1 (*Continued*)

| Molecule | Solvent conditions | Specific volume[a] | | Hydration[b] | | |
|---|---|---|---|---|---|---|
| | | $\bar{v}$ ($cm^3\ g^{-1}$) | Reference[d] | $\delta_1$ ($g\ g^{-1}$) | Method[c] | Reference[d] |
| | | | | 0.57 | Hydrodynamic | [5] |
| | | | | 0.28 | Calc. | [84] |
| | | | | 0.335 | Calc.[g] | [3,55] |
| | | | | 0.36 | Calc. | [3,55] |
| | | | | 0.35 | Calc.[e] | This study |
| Malate dehydrogenase, halophilic | NaCl | 0.73 | [87] | 0.35–0.45 | Thermodynamic | [15,87] |
| | | | | 0.252 | Calc. | [15] |
| Default value for simple proteins | | | | 0.14–1.04 | Hydrodynamic | [81] |
| | | | | 0.2–0.35 | | [88] |
| | | | | 0.2–0.4 | | [87] |
| | | | | 0.25 | | [89] |
| | | | | 0.3 | | [34] |
| | | | | 0.3–0.4 | | [81] |
| | | | | 0.3–0.5 | | [90] |
| | | 0.735 | [40] | 0.35 | | [40,53] |
| | | | | $0.36 \pm 0.04$ | NMR | [5,55] |
| | | 0.730 | [5] | $0.53 \pm 0.26$ | | [5] |
| Monomeric proteins ($M < 100\ kg\ mol^{-1}$) | | | | 0.280 | | [23,56,57] |
| Oligomeric proteins ($M > 100\ kg\ mol^{-1}$) | | | | 0.444 | | [23,56,57] |
| *2. Glycoproteins:* | | | | | | |
| Fibronectin (human) | | 0.72 | [40] | 0.64 | SAXS | [40] |
| Fibrinogen (bovine) | | | | 0.5 | Hydrodynamic | [3] |
| | | 0.700 | [58] | 4.45 | SAXS | [41] |
| Mucus glycoprotein (human) | | 0.633 | [91] | 100 | Hydrodynamic | [53] |
| Default value for glycoproteins | | | | 0.3 | | [78,92] |
| *3. Polysaccharides:* | | | | | | |
| Dextran | | 0.620[h] | [39] | 0.2 | NMR | [93] |
| Sephadex | | | | 0.3 | NMR | [90] |
| Default value for polysaccharides | | | | 0.1–0.2 | NMR | [93] |
| *4. Nucleoproteins, viruses:* | | | | | | |
| Bacteriophage fr | | 0.673 | [40] | 0.91 | SAXS | [40] |
| Tomato bushy stunt virus | | 0.700 | [40] | 0.99 | SAXS | [40] |

Table 1 (*Continued*)

| Molecule | Solvent conditions | Specific volume[a] | | Hydration[b] | | |
|---|---|---|---|---|---|---|
| | | $\bar{v}$ ($cm^3\ g^{-1}$) | Reference[d] | $\delta_1$ ($g\ g^{-1}$) | Method[c] | Reference[d] |
| *5. Nucleic Acids:* | | | | | | |
| DNA | | | | 0.35–1.6 | Different | [93] |
| | | | | 0.59 | NMR | [3] |
| | | | | 0.61 | Calorimetric | [3] |
| | | | | 1.5 | NMR | [93] |
| | 1 M NaCl | 0.528 | [85] | 0.20 | Thermodynamic | [15,85] |
| | CsCl | | | 0.24 | Thermodynamic | [15] |
| Denatured | | | | 0.65 | Calorimetric | [3] |
| t-RNA | | 0.54 | [40] | 0.34 | SAXS | [40] |
| Denatured | | | | 1.7 | NMR | [90] |
| 5S rRNA | | 0.54 | [40] | 0.23 | SAXS | [40] |

The values are valid for aqueous solutions (water or dilute buffer, unless otherwise stated) at 20–25°C.

[a] Partial specific volume, $\bar{v}$, obtained preferably by densimetry (for details see: [36,39]).

[b] Hydration, $\delta_1$, in grams of water per gram of molecule under analysis.

[c] Thermodynamic analysis based primarily on densimetry (preferential binding of water).

[d] Detailed citations can be found in the references given.

[e] Based on the sequence deposited in the SWISS-PROT data bank [94]: accession numbers P02769, P00432, P00889, and P00698 for albumin, catalase, citrate synthase, and lysozyme, respectively. For calculations all amino acid residues are used, irrespective of their localization in the protein interior or outside (exposed to the solvent).

[f] Corrected for ligands (heme b, $NADPH_2$).

[g] Corrected for buried residues.

[h] For $\bar{v}$ the value for the monomeric unit (glucose) was used.

scattering, and modeling, the exact value of the partial molar or partial specific volume ($\overline{V}$, $\bar{v}$) and/or other volume quantities is a necessary prerequisite. In the case of biomolecules, the densimetric exploration of isomolal or isopotential volume quantities is straightforward [36,39]. In the case of simple proteins, the average value for $\bar{v}$ is approximately 0.735 $cm^3\ g^{-1}$ and does not exhibit pronounced scatter (Fig. 1; Table 1).

If the experimental determination of $\overline{V}$ or $\bar{v}$ is not feasible (e.g. because of a lack of material, insufficient solubility, strong adsorption behavior), experiments have to be replaced with appropriate calculations. This is demonstrated in Fig. 2 for the two ligands of catalase, heme b and $NADPH_2$, their $\overline{V}$ values being required for modeling purposes (see Section 3.2). The validity of this approach [37,38] has been demonstrated for numerous substances of quite different properties (including hydration): compounds like $NAD^+$, NADH, acetyl-coenzyme A (free acids, anions, salts).

As follows from the experiments and compilations of many authors (e.g. [2,3,5,9,15,19,23,40,41,55]), the application of various physicochemical techniques to biological molecules yields hydration values, $\delta_1$ (in grams of water per gram of molecule), varying over a wide range (Table 1). The values vary for different classes of compounds (non-conjugated and conjugated proteins, nucleic acids, polysaccharides, etc.) and environmental conditions [e.g. presence of high concentrations of third components (co-solvents, denaturants, etc.)]. The vast majority of values have been reported for simple proteins in aqueous solution ($c$ of co-solvents $< 0.2$ M) which, as a first approximation, can be regarded as two-component systems. Experimental results found for proteins are also compared to predictions from the sequence: $\delta_1$ values calculated according to Kuntz

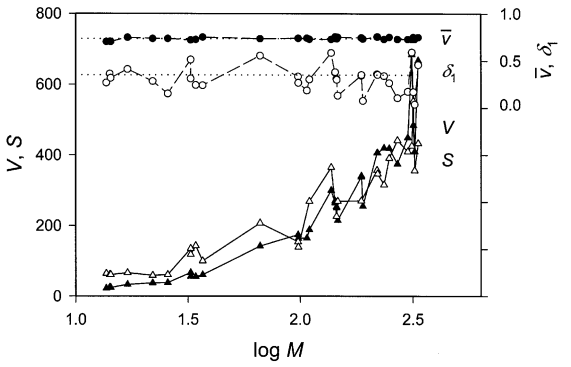


Fig. 1. Experimental values for hydrated volume (▲), $V$ (in $nm^3$), surface area (△), $S$ (in $nm^2$), partial specific volume (●), $\bar{v}$ (in $cm^3\ g^{-1}$), and hydration (○), $\delta_1$ (in grams of water per gram of biopolymer) of 34 selected simple proteins plotted as a function of the logarithm of molar mass, $M$ (in kg $mol^{-1}$), as derived from SAXS ($V$, $S$, $\delta_1$) and densimetry ($\bar{v}$), respectively. Default values for $\bar{v}$ (0.735 $cm^3\ g^{-1}$) and $\delta_1$ (0.35 g $g^{-1}$) are shown as dotted lines. For details of measurements and observed values see [40,41,52].

[55] agree satisfactorily with experimental values, though their pH dependence should be taken into account (cf. Table 1: albumin). Calculated values may be applied for various purposes, e.g. for the calculation of isopotential specific volumes of proteins in high concentrations of denaturing agents (6 M guanidinium chloride, 8 M urea) from increments (cf. [36,39] and references therein), or for modeling purposes as shown in this study.

For molecules possessing average properties, e.g. simple globular proteins, reasonable average values for $\delta_1$ can be derived from experimental determinations. As an example, the hydration values obtained from the hydrated particle volumes by means of SAXS are illustrated in more detail. The hydration values obtained show a strong scatter (Fig. 1), obviously due to deficiencies in the determination of the SAXS volumes required for the $\delta_1$ estimates. The deviations for the $\delta_1$ values coincide exactly with the deviations found for $V$ and $S$.

From SAXS of the apo- and holoforms of 34 simple proteins ($M = 14$–$333$ kg $mol^{-1}$, axial ratio $p = 0.2$–$5$; Fig. 1) an average hydration value of $0.31 \pm 0.14$ g $g^{-1}$ can be deduced, if the density of bound water is taken as 1 g $cm^{-3}$ (as done in the past by most authors).[4] This result is in agreement with $0.32 \pm 0.13$ g $g^{-1}$ obtained earlier for a set of 21 simple apoproteins [40]. Average values between 0.34 or 0.38 g $g^{-1}$, however, would be gained for the 34 proteins mentioned, if an increase in water density of 10 or 20% [18,26,77–79] is assumed. Similar average values as obtained by SAXS have been obtained from other techniques, though the accuracy that can be achieved by different methods is quite different and though differing protein sets have been used.

The experimental determination of $\delta_1$ is difficult and the results seem to depend on the technique applied. According to the literature, the hydrodynamic hydration of proteins often exceeds the hydration obtained by other methods ([5]; cf. Table 1). While the majority of SAXS experiments yield results consistent with other techniques, a few examples of SAXS studies (e.g. [80]) seem to underestimate the hydration. In the context of the mentioned discrepancies, however, the question arises to what extent the results are caused/influenced by the assumptions underlying the evaluation and interpretation of the data (e.g. uncritical modeling by ellipsoids of revolution; cf. [81]). On the other hand, whole-body modeling, based on $V$ and $R_G$ or $s$ and $D$ of a variety of biopolymers, showed full compatibility between SAXS and hydrodynamic data [40,41,49,58], without involving extreme values for $\delta_1$. This suggests that appropriate data treatment and modeling are more important for the determination of $\delta_1$ than the choice of the experimental technique.

In the case of lacking databases for hydration values, default values may be used instead, especially for molecules with average properties. For simple proteins, for a good approximation, a $\delta_1$ value of 0.35 g water/g protein may be applied (Fig. 1; Table 1).

[4] The use of a value of 1 g $cm^{-3}$ for the density of hydration water goes back to the early beginnings of SAXS when the difference between $V$ and $V_{dry}$ was attributed to an 'inner solvation' of the biopolymers. Actually a hydration shell can only be detected by SAXS if the shell has a density different from that of the surrounding bulk water to give a significant electron density contrast.

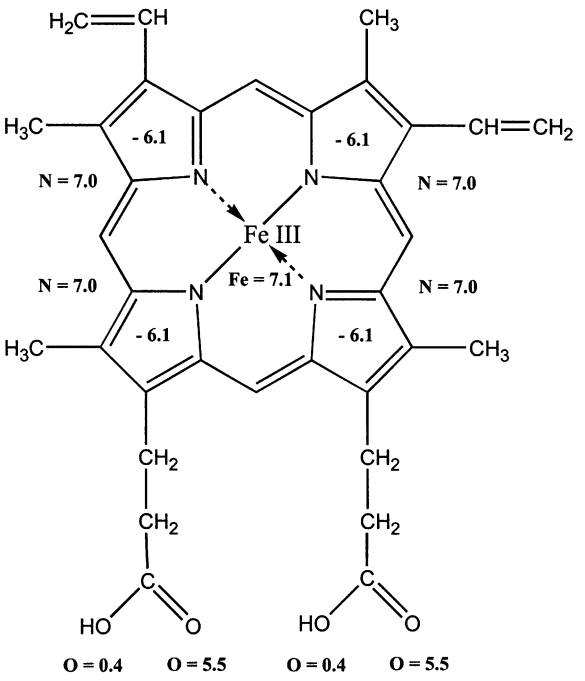


**Heme b**

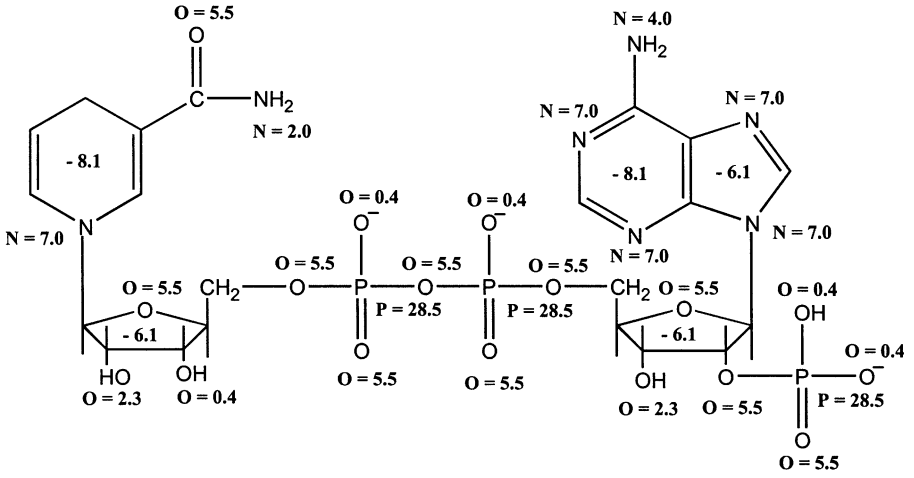


**$NADPH_2$**

Fig. 2. Calculation of the partial specific volume of the ligands of catalase, heme b and $NADPH_2$, from volume increments for atoms according to [37,38]. The values for N and O which depend on the neighborhood are indicated in the figure, together with the values for P and Fe. Heme b: $C_{34}H_{32}N_4O_4Fe$: $M = 616.50$ g mol$^{-1}$; $\overline{V}_c = 34 \times 9.9$ (C) $+ 32 \times 3.1$ (H) $+ 4 \times 7.0$ (N) $+ 2 \times 0.4$ (O) $+ 2 \times 5.5$ (O) $+ 7.1$ (Fe) $+ 12.4$ ($V_{CV}$) $- 4 \times 6.1$ ($V_{RF}$) $= 470.7$ cm$^3$ mol$^{-1}$; $\bar{v}_c = \overline{V}_c/M = 0.7635$ cm$^3$ g$^{-1}$. $NADPH_2$ (trianion): $C_{21}H_{27}N_7O_{17}P_3$; $M = 742.40$ g mol$^{-1}$; $\overline{V}_c = 21 \times 9.9$ (C) $+ 27 \times 3.1$ (H) $+ 1 \times 2.0$ (N) $+ 1 \times 4.0$ (N) $+ 5 \times 7.0$ (N) $+ 5 \times 0.4$ (O) $+ 2 \times 2.3$ (O) $+ 10 \times 5.5$ (O) $+ 3 \times 28.5$ (P) $+ 12.4$ ($V_{CV}$) $- 2 \times 8.1$ ($V_{RF}$) $- 3 \times 6.1$ ($V_{RF}$) $- 3 \times 6.7$ ($V_{ES^-}$) $= 437.5$ cm$^3$ mol$^{-1}$; $\bar{v}_c = \overline{V}_c/M = 0.5893$ cm$^3$ g$^{-1}$.

### 3.2. Modeling approaches

Using the tetrameric enzyme catalase, a variety of models were constructed. The results of possible approaches to predict structural and hydrodynamic data are given in Table 2 for two extreme cases of volume, $V_{HOH}$, of bound water molecules. Some selected initial and reduced models are illustrated in Fig. 3. The molecular features of the reduced models correspond to those of the initial models.

For predictions, the following molecular parameters were used: volume, $V$, radius of gyration, $R_G$, sedimentation coefficient, $s$, diffusion coefficient, $D$, and intrinsic viscosity [η]. Predicted values were compared with experimental

Table 2
Comparison of experimental and calculated structural and hydrodynamic parameters of bovine liver catalase

| | $N_{HOH}$ | $\delta_1$ (g/g) | $N_{Beads}$[a] | V ($nm^3$) | $R_{G,SAXS}$[a,b] (nm) | $R_{G,Hydro}$[c] (nm) | $s \times 10^{13}$ (s) | $D \times 10^7$ ($cm^2/s$) | [η] ($cm^3/g$) |
|---|---|---|---|---|---|---|---|---|---|
| Experimental, native enzyme[d] | | | | 420.0[e] | 3.68[f] | | 11.3[h] | 4.1[h] | 3.9[i] |
| | | | | | 3.98[g] | | 11.6[i] | 4.5[j] | |
| Model 1: 8CAT, anhydrous protein[k] | 0 | 0 | 2000 | 278.7 | 3.62 | | | | |
| | | | 434 | | 3.61 | 3.60 | 12.38 | 4.74 | 2.47 |
| Model 2: Kuntz hydration of all AA | 5060 | 0.387 | 2000 | 402.7 | 3.63 | | | | |
| ($V_{HOH}$ = 0.0245 $nm^3$; expanded AA) | | | 434 | | 3.63 | 3.62 | 12.15 | 4.65 | 2.61 |
| Model 3: Kuntz hydration of all AA | 5060 | 0.387 | 2000 | 422.4 | 3.62 | | | | |
| ($V_{HOH}$ = 0.0284 $nm^3$; expanded AA) | | | 434 | | 3.62 | 3.62 | 12.12 | 4.64 | 2.63 |
| Model 4: low hydration of accessible AA | 3026 | 0.231 | 5026 | 352.9 | 3.69 | | | | |
| (SIMS; $V_{HOH}$ = 0.0245 $nm^3$) | | | 578 | | 3.69 | 3.70 | 11.81 | 4.52 | 2.84 |
| Model 5: max. hydration of accessible AA | 4048 | 0.309 | 6048 | 377.9 | 3.74 | | | | |
| (SIMS; $V_{HOH}$ = 0.0245 $nm^3$) | | | 630 | | 3.73 | 3.76 | 11.60 | 4.44 | 3.01 |
| Model 6: low hydration of accessible AA | 3026 | 0.231 | 5026 | 364.7 | 3.64 | | | | |
| (SIMS; $V_{HOH}$ = 0.0284 $nm^3$) | | | 578 | | 3.65 | 3.72 | 11.78 | 4.51 | 2.87 |
| Model 7: max. hydration of accessible AA | 4048 | 0.309 | 6048 | 393.7 | 3.66 | | | | |
| (SIMS; $V_{HOH}$ = 0.0284 $nm^3$) | | | 630 | | 3.67 | 3.78 | 11.56 | 4.42 | 3.04 |
| Model 8: low hydration of accessible AA | 2930 | 0.224 | 4930 | 350.5 | 3.69 | | | | |
| (MSRoll; $V_{HOH}$ = 0.0245 $nm^3$) | | | 596 | | 3.69 | 3.71 | 11.81 | 4.52 | 2.84 |
| Model 9: max. hydration of accessible AA | 3897 | 0.298 | 5897 | 374.2 | 3.74 | | | | |
| (MSRoll; $V_{HOH}$ = 0.0245 $nm^3$) | | | 631 | | 3.73 | 3.76 | 11.58 | 4.43 | 3.02 |
| Model 10: low hydration of accessible AA | 2930 | 0.224 | 4930 | 361.9 | 3.64 | | | | |
| (MSRoll; $V_{HOH}$ = 0.0284 $nm^3$) | | | 596 | | 3.65 | 3.72 | 11.78 | 4.51 | 2.87 |
| Model 11: max. hydration of accessible AA | 3897 | 0.298 | 5897 | 389.4 | 3.66 | | | | |
| (MSRoll; $V_{HOH}$ = 0.0284 $nm^3$) | | | 631 | | 3.67 | 3.78 | 11.54 | 4.42 | 3.05 |
| Model 12: low hydration of accessible AA | 3026 | 0.231 | 2000 | 352.9 | 3.69 | | | | |
| (SIMS; $V_{HOH}$ = 0.0245 $nm^3$; expanded AA) | | | 468 | | 3.68 | 3.69 | 12.02 | 4.60 | 2.70 |
| Model 13: max. hydration of accessible AA | 4048 | 0.309 | 2000 | 377.9 | 3.73 | | | | |
| (SIMS; $V_{HOH}$ = 0.0245 $nm^3$; expanded AA) | | | 482 | | 3.73 | 3.75 | 11.78 | 4.51 | 2.87 |
| Model 14: low hydration of accessible AA | 3026 | 0.231 | 2000 | 364.7 | 3.64 | | | | |
| (SIMS; $V_{HOH}$ = 0.0284 $nm^3$; expanded AA) | | | 454 | | 3.64 | 3.69 | 12.08 | 4.62 | 2.66 |
| Model 15: max. hydration of accessible AA | 4048 | 0.309 | 2000 | 393.7 | 3.66 | | | | |
| (SIMS; $V_{HOH}$ = 0.0284 $nm^3$; expanded AA) | | | 456 | | 3.66 | 3.75 | 11.90 | 4.55 | 2.78 |

[a] The value in the first line refers to the initial (hydrated) model, and that in the second line to the reduced model.
[b] Radius of gyration calculated from the radii, coordinates, and the number of excess electrons of the beads.
[c] Radius of gyration calculated from the radii and coordinates.
[d] Molar mass $M$ = 235.8 kg /mol (mass of the apoenzyme as derived from the SWISS-PROT data bank [94] plus masses of the ligands, heme b and $NADPH_2$); partial specific volume $\bar{v}$ = 0.730 $cm^3/g$ [95].
[e] Ref. [48].
[f] Ref. [44].
[g] Ref. [43].
[h] Ref. [45].
[i] Ref. [46].
[j] Ref. [47].
[k] The model includes the contributions of the ligands, however, a few terminal amino acids are missing in the crystal structure.

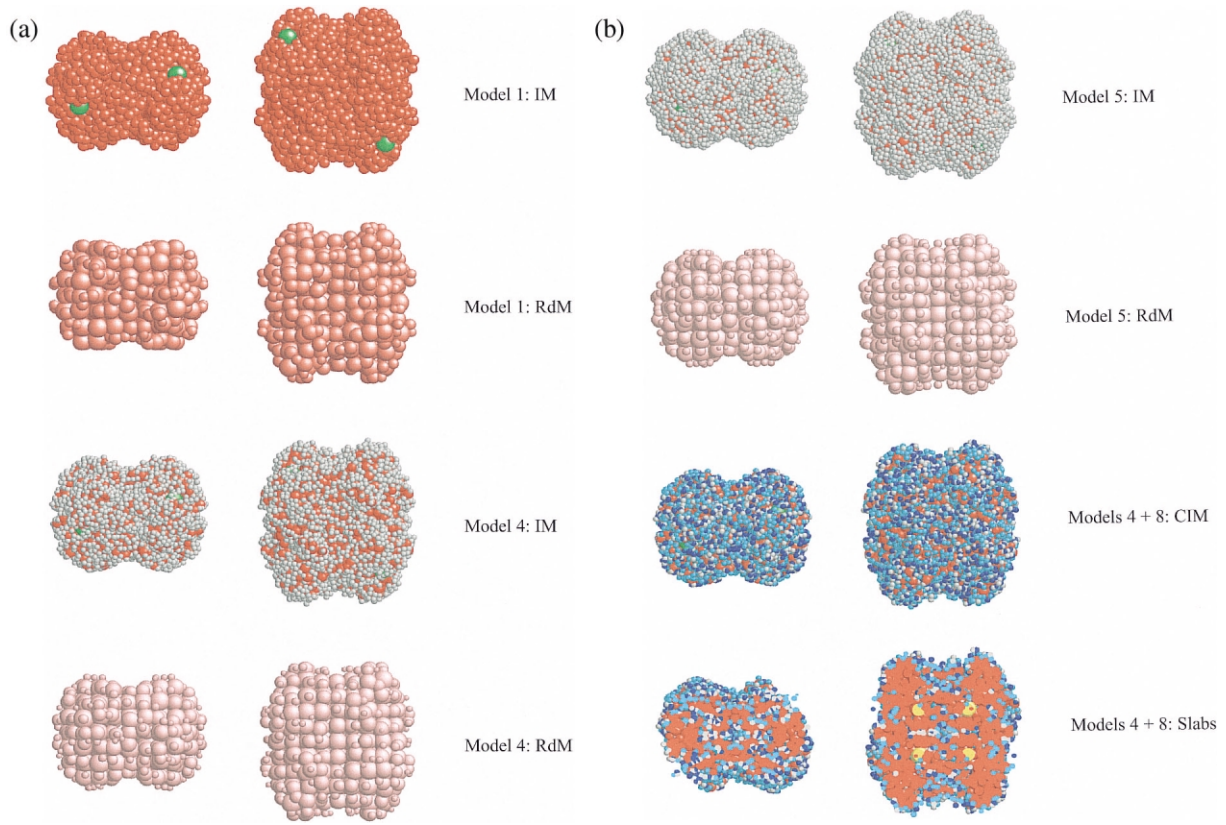


Fig. 3. Side and top views of selected hydrodynamic models for catalase: (i) initial models (IM) obtained from the PDB file 8CAT (converting the atomic coordinates to coordinates of the amino acid residues and the ligands, heme b and $NADPH_2$); (ii) reduced models (RdM) derived therefrom; and (iii) a comparison of initial models (CIM) obtained from application of the surface dot points of program SIMS or MSRoll, respectively, together with central slabs. The basic molecular components are shown in different colors: red, amino acid residues; green, $NADPH_2$; yellow, heme b; gray and blue, bound water molecules based on programs SIMS or MSRoll, respectively; water molecules which are common to both SIMS and MSRoll models (overlapping more than 50% of their volume) are highlighted in cyan. Further details of the respective models are explained in Table 2. Graphics were made with the program RasMol [96].

data derived from various sources. On the basis of the present results, for $R_G$ the lower experimental value of 3.68 nm [44] should be preferred, since the higher value of 3.98 nm [43] is obviously incompatible with all calculated data given in Table 2. Presumably the presence of aggregates was responsible for the $R_G$ of 3.98 nm, since the author has found a maximum particle diameter of 14.6 nm [43] which evidently disagrees with the diameter derived from the crystal structure (cf. Figs. 4 and 5).

As may be taken from the results for $[\eta]$ in Table 2, none of the predicted values is compatible with the experimental value. Possible explanations for this discrepancy are shortcomings of the existing approaches for predictions of $[\eta]$, including inadequate volume corrections (cf. [32,35,82,83]), and experimental deficiencies. Already in the case of whole-body approaches, $[\eta]$ has turned out to be a rather unreliable experimental parameter [40]. For the mentioned reasons, we abstain from further interpretations of the $[\eta]$ values in Table 2.

We started our modeling approaches with the dry (anhydrous) protein (model 1) consisting of amino acid residues and the ligands, heme b and

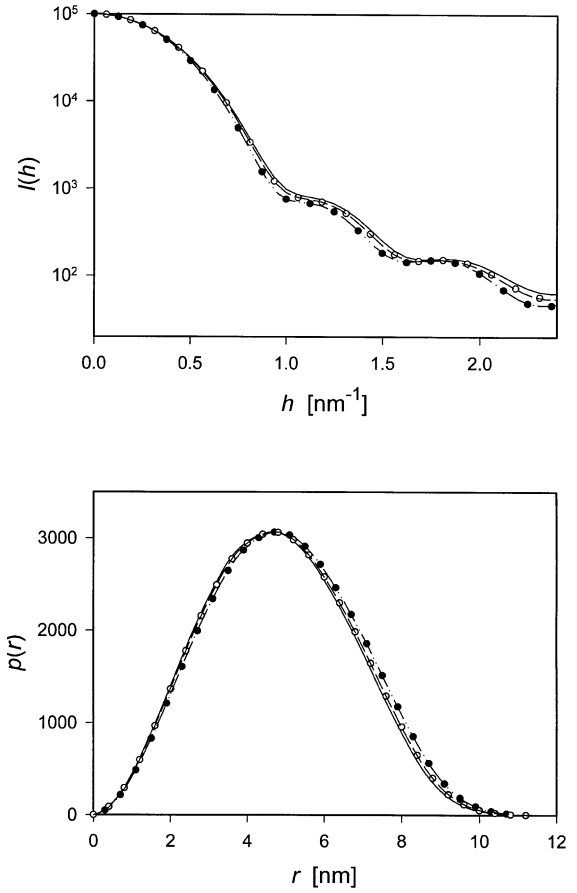


Fig. 4. Scattering curves, $I(h)$, and pair–distance distribution functions, $p(r)$, of selected hydrodynamic models for catalase given in Fig. 3 and Table 2, where $h = 4\pi\sin\theta/\lambda$ ($2\theta$ = scattering angle, $\lambda$ = wavelength) and $r$ is the distance between two arbitrarily chosen points (electrons) within the molecule. For better comparison, the $p(r)$ functions have been normalized to the same height of the maximum. The selected models comprise a few representative examples (IM, $V_{HOH} = 0.0245$ or $0.0284$ nm$^3$): the anhydrous protein (model 1: ——); maximum hydration at selected SIMS points (model 5: ●, $V_{HOH} = 0.0245$ nm$^3$; model 7: ○, $V_{HOH} = 0.0284$ nm$^3$; model 13: — ·· —, $V_{HOH} = 0.0245$ nm$^3$, expanded AA; model 15: — — —, $V_{HOH} = 0.0284$ nm$^3$, expanded AA). While initial and reduced models exhibit only marginal differences (not shown), the results for different densities of bound water diverge significantly: both $I(h)$ and $p(r)$ found for $V_{HOH} = 0.0245$ nm$^3$ result in the most pronounced deviations, if compared to the anhydrous protein. The values obtained for the Kuntz hydration of all amino acid residues (models 2 and 3) yield curves similar to the anhydrous protein (not shown).

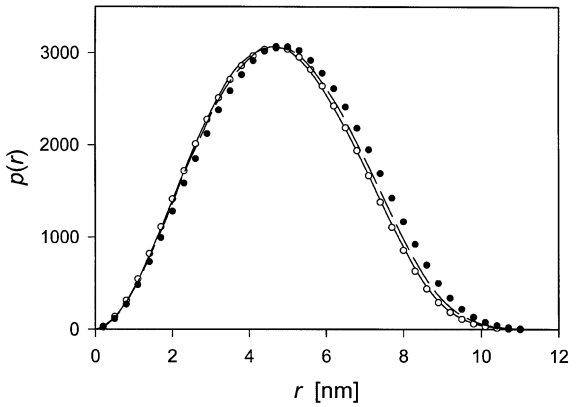


Fig. 5. Pair–distance distribution functions, $p(r)$, of selected hydrodynamic models for catalase given in Fig. 3 and Table 2, to illustrate differences in the results of the calculations based on mass points or excess electrons, where $r$ is the distance between mass points (symbols) or electrons (lines), respectively. For clarity, the figure comprises only model 1 (○ and ———, anhydrous protein, IM) and model 7 (● and — — —, maximum hydration at selected SIMS points, $V_{HOH} = 0.0284$ nm$^3$, RdM). In the case of hydrated proteins, the figure shows marked deviations between these two types of functions: the frequency of larger distances of the hydrodynamic $p(r)$ functions is increased, if compared to the functions based on excess electrons. In the case of the anhydrous protein, only marginal differences (in the opposite direction) can be found.

$NADPH_2$. Only two out of four $NADPH_2$ molecules are visible simultaneously, the remaining two are located at the back side. The four heme b ligands are located in the protein interior, but can be visualized in the slabs. To enable hydrodynamic calculations, we then reduced the number of beads ($2000 \rightarrow 434$). The predictions, with respect to $V$, $R_G$, $s$ and $D$, obviously failed, if compared to the experimental data.

The simplest possibility to give correct values for $V$ and/or $R_G$ would be to expand the whole molecule by applying transformation factors acting on bead radii and/or coordinates [31,32]. This procedure, however, involves some problems [35] and requires knowledge of the values for $V$ and $R_G$ to be simulated. The alternate assumption of definite hydration values for all amino acid residues (AA) according to Kuntz [55] also blows

up the molecule. In this case, different expansion factors have to be applied to different types of residues, to give appropriate results concerning $V$ (models 2 and 3).

When using the programs SIMS and MSRoll, many dot surface points are created which may be used as starting points for the localization of bound water molecules. To obtain correct values for $V$, $R_G$, and hydrodynamic parameters, we have to modulate the number of beads corresponding to different amounts of hydration (models 4–7 and 8–11). The application of both programs yields similar results. In particular, the assumption of maximum hydration for the accessible amino acid residues, i.e. production of a more pronounced, but not uniform water shell, results in good parameter predictions. In an alternative approach, we hydrated all accessible AA (data not shown), i.e. including Phe (which according to Kuntz [55] has no hydration): this procedure resulted in a slightly enhanced maximum hydration ($\Delta\delta_1 = 0.003–0.004$ g/g). A further calculation alternative, an expansion of amino acid residues on the protein surface, is demonstrated for the models based on the program SIMS (models 12–15).

Since use of the programs SIMS and MSRoll, together with our hydration algorithms, results in similar predictions, it was of interest to compare the number and positions of the water molecules created by these two efficient surface calculation programs under similar constraints (Fig. 3: model 4 vs. model 8). Though the water molecules are located at slightly different positions, their number, and the predicted structural and hydrodynamic results, are similar (1789 water molecules, which overlap with more than 50% of their volume, may, however, be assigned to both models). As long as we are concerned with time-averaged protein properties, this finding obviously is satisfactory, since there is always a time-dependent fluctuation of the water molecules 'bound' to a protein.

From our computer simulations follows the interesting conclusion that there are also water molecules inside catalase, at least in some cavities and channels leading to the position of the four heme groups. This feature is caused by the biochemical function of the heme groups and is no contradiction to the well-known fact that, in general, no space is left for water molecules inside the protein interior.

In addition to the visual inspection of the models (Fig. 3) and the quantitative comparison of observed and predicted hydrodynamic parameters (Table 2), we derived the SAXS functions, $I(h)$ and $p(r)$, to test the influence of the applied data reduction approaches and the influence of various hydration contributions reflected by the models. The functions for initial and reduced models are virtually identical, thus proving the correctness of the performed data reductions. In the case of catalase, all functions resemble each other to some extent (Fig. 4); however, models without hydration (model 1), models assuming a Kuntz hydration for all AA (models 2 and 3), and models based on unrealistic (too low or too high) numbers of water molecules may be excluded. On the basis of the present results for catalase, no clear-cut decision between the values to be used for the density of bound water can be made. Approximately 4000 water molecules are bound to the protein, most of them covering the protein surface.

An interesting observation is the fact that the $p(r)$ functions of models based on the number of excess electrons are clearly different from the 'hydrodynamic' functions based on mass points (Fig. 5). This finding is a point of special importance, if details of data (e.g. concerning the shape of the $p(r)$ function, the exact value of $R_G$, etc.) are to be compared. A critical inspection of the $R_G$ values calculated on the basis of excess electrons or mass points reveals slight discrepancies between these two types of $R_G$ values, especially if maximum hydration is assumed (Table 2).

## 4. Conclusions

In the context of the behavior of proteins or other biopolymers in solution, one of the crucial problems is hydration. To handle this problem in an appropriate manner, we have tried to simulate the behavior of bound water molecules using quite different approaches. Of course, we could not

apply the water molecules seen by crystallographers, since, in general, only a few water molecules are localized in fixed positions (and not necessarily at positions relevant for the solution behavior). Their number is too low to represent the water responsible for hydrodynamic hydration.

For the simulation of the water molecules on the protein surface, we have used a variety of surface calculation approaches, in order to test the number, position and density/volume of bound water molecules. There is no doubt that water molecules do not surround proteins as a uniform shell. Although in the case of simple, non-conjugated (soluble) proteins, the majority of polar (hydrophilic) AA are located on the protein surface, and therefore, are preferred targets of water binding, there are also several hydrophobic patches on the protein surface. This can also be visualized from Fig. 3 (e.g. model 4: IM) and has been taken into account by our hydration algorithms.

Summarizing our results, we may state that we are able to realistically simulate the amount and time-averaged positions of water molecules on a protein surface. On the basis of computer simulations, both the scattering and hydrodynamic behavior is anticipated efficaciously, if appropriate hydration contributions are taken into account. At present, however, a series of problems remain. In the case of catalase: (i) parameters and scattering functions seem to be very similar irrespective of the extent of hydration; and (ii) no experimental scattering curve covering the whole angular range is available. The first deficit may be caused by the large mass and the oblate shape of this protein, the second one requires the measurement of very accurate scattering curves for catalase in the future. The only available experimental scattering curve for catalase [44] covers only part of the theoretical scattering curve. It is, within the accuracy of experimental data, compatible with the curves of the hydrated models shown in Fig. 4, but, however, does not allow a final decision concerning the total amount and the precise density of bound water. Anyhow, further, very detailed SAXS experiments on catalase and other proteins and other types of biopolymers of quite different shape and composition of subunits are required, before final statements or generalizations concerning hydration contributions can be made.

A computer program implementing the hydration algorithm will be available upon request in the near future.

## Acknowledgements

We are grateful to Y.N. Vorobjev for making the SIMS program available to us, to J. García de la Torre for the HYDRO program, and to J.F. Díaz for providing the experimental scattering curve of catalase.

## References

[1] A.G. Ogston, On water binding, Fed. Proc. 25 (1966) 986–989.
[2] G.N. Ling, Hydration of macromolecules in: R.A. Horne (Ed.), Water and Aqueous Solutions, Wiley Interscience, New York, 1972, pp. 663–700.
[3] I.D. Kuntz Jr., W. Kauzmann, Hydration of proteins and polypeptides, Adv. Protein Chem. 28 (1974) 239–345.
[4] A.J. Hopfinger, Intermolecular Interactions and Biomolecular Organizations, John Wiley & Sons, New York, 1977.
[5] P.G. Squire, M.E. Himmel, Hydrodynamics and protein hydration, Arch. Biochem. Biophys. 196 (1979) 165–177.
[6] B.E. Conway, Ionic Hydration in Chemistry and Biophysics, Elsevier, Amsterdam, 1981.
[7] F. Franks, S. Mathias (Eds.), Biophysics of Water, John Wiley & Sons, Chichester, 1982.
[8] N. Thanki, J.M. Thornton, J.M. Goodfellow, Distributions of water around amino acid residues in proteins, J. Mol. Biol. 202 (1988) 637–657.
[9] S.N. Timasheff, T. Arakawa, Stabilization of protein structure by solvents in: T.E. Creighton (Ed.), Protein Structure: A Practical Approach, IRL Press, Oxford, 1989, pp. 331–345.
[10] A. Ben-Naim, Solvent effects on protein association and protein folding, Biopolymers 29 (1990) 567–596.
[11] J.A. Rupley, G. Careri, Protein hydration and function, Adv. Protein Chem. 41 (1991) 37–172.
[12] M. Oobatake, T. Ooi, Hydration and heat stability effects on protein unfolding, Progr. Biophys. Molec. Biol. 59 (1993) 237–284.
[13] M. Levitt, B.H. Park, Water: now you see it, now you don't, Structure 1 (1993) 223–226.
[14] E. Westhof (Ed.), Water and Biological Macromolecules, Macmillan, London, 1993.

[15] H. Eisenberg, Protein and nucleic acid hydration and cosolvent interactions: establishment of reliable baseline values at high cosolvent concentrations, Biophys. Chem. 53 (1994) 57–68.

[16] A.A. Rashin (Ed.), Special issue: thermodynamics of hydration, Biophys. Chem. 51 (1994) 89–417.

[17] R.B. Gregory (Ed.), Protein–Solvent Interactions, Marcel Dekker, New York, 1995.

[18] M. Gerstein, C. Chothia, Packing at the protein–water interface, Proc. Natl. Acad. Sci. USA 93 (1996) 10167–10172.

[19] S.N. Timasheff, Control of protein stability and reactions by weakly interacting cosolvents: the simplicity of the complicated, Adv. Protein Chem. 51 (1998) 355–432.

[20] J.C. Lee, K. Gekko, S.N. Timasheff, Measurements of preferential solvent interactions by densimetric techniques, Methods Enzymol. 61 (1979) 26–49.

[21] D.L. Vandermeulen, N. Ressler, A near-infrared analysis of water-macromolecule interactions: hydration and the spectra of aqueous solutions of intact proteins, Arch. Biochem. Biophys. 199 (1980) 197–205.

[22] S. Bone, R. Pethig, Dielectric studies of protein hydration and hydration-induced flexibility, J. Mol. Biol. 181 (1985) 323–326.

[23] H. Pessen, T.F. Kumosinski, Measurements of protein hydration by various techniques, Methods Enzymol. 117 (1985) 219–255.

[24] M. Lüscher-Mattli, Thermodynamic parameters of biopolymer–water systems, in: H.-J. Hinz (Ed.), Thermodynamic Data for Biochemistry and Biotechnology, Springer-Verlag, Berlin, 1986, pp. 276–294.

[25] G. Otting, E. Liepinsh, K. Wüthrich, Protein hydration in aqueous solution, Science 254 (1991) 974–980.

[26] D.I. Svergun, S. Richard, M.H.J. Koch, Z. Sayers, S. Kuprin, G. Zaccai, Protein hydration in solution: experimental observation by X-ray and neutron scattering, Proc. Natl. Acad. Sci. USA 95 (1998) 2267–2272.

[27] K.F. Smith, R.A. Harrison, S.J. Perkins, Structural comparisons of the native and reactive-centre-cleaved forms of $\alpha_1$-antitrypsin by neutron- and X-ray-scattering in solution, Biochem. J. 267 (1990) 203–212.

[28] A.J. Beavil, R.J. Young, B.J. Sutton, S.J. Perkins, Bent domain structure of recombinant IgE-Fc in solution by X-ray and neutron scattering in conjunction with an automated curve fitting procedure, Biochemistry 34 (1995) 14449–14461.

[29] A.W. Ashton, M.K. Boehm, J.R. Gallimore, M.B. Pepys, S.J. Perkins, Pentameric and decameric structures in solution of serum amyloid P component by X-ray and neutron scattering and molecular modelling analyses, J. Mol. Biol. 272 (1997) 408–422.

[30] O. Byron, Construction of hydrodynamic bead models from high-resolution X-ray crystallographic or nuclear magnetic resonance data, Biophys. J. 72 (1997) 408–415.

[31] P. Zipper, H. Durchschlag, Calculation of hydrodynamic parameters of proteins from crystallographic data using multibody approaches, Progr. Colloid Polym. Sci. 107 (1997) 58–71.

[32] P. Zipper, H. Durchschlag, Recent advances in the calculation of hydrodynamic parameters from crystallographic data by multibody approaches, Biochem. Soc. Trans. 26 (1998) 726–731.

[33] P. Zipper, H. Durchschlag, Prediction of hydrodynamic and small-angle scattering parameters from crystal and electron microscopic structures, J. Appl. Cryst. 33 (2000) 788–792.

[34] O. Byron, Hydrodynamic bead modeling of biological macromolecules, Methods Enzymol. 321 (2000) 278–304.

[35] J. García de la Torre, M.L. Huertas, B. Carrasco, Calculation of hydrodynamic properties of globular proteins from their atomic-level structure, Biophys. J. 78 (2000) 719–730.

[36] H. Durchschlag, Specific volumes of biological macromolecules and some other molecules of biological interest, in: H.-J. Hinz (Ed.), Thermodynamic Data for Biochemistry and Biotechnology, Springer-Verlag, Berlin, 1986, pp. 45–128.

[37] H. Durchschlag, P. Zipper, Calculation of the partial specific volume of organic compounds and polymers, Progr. Colloid Polym. Sci. 94 (1994) 20–39.

[38] H. Durchschlag, P. Zipper, Calculation of partial specific volumes and other volumetric properties of small molecules and polymers, J. Appl. Cryst. 30 (1997) 803–807.

[39] H. Durchschlag, Partial specific volumes and other volumetric properties of proteins and substances related to protein chemistry, in: H.-J. Hinz (Ed.), Landolt-Börnstein New Series VII/2A, Springer-Verlag, Berlin, 2001. in press

[40] H. Durchschlag, P. Zipper, Calculation of structural parameters from hydrodynamic data, Progr. Colloid Polym. Sci. 113 (1999) 87–105.

[41] H. Durchschlag, P. Zipper, Correlations between crystallographic, small-angle scattering and hydrodynamic data of biopolymers, Progr. Colloid Polym. Sci. (2001) in press.

[42] I. Fita, M.R.N. Murthy, M.G. Rossmann, A.M. Silva, The refined structure of beef liver catalase at 2.5 Å resolution, Acta Cryst. B42 (1986) 497–515.

[43] A.G. Malmon, Small angle X-ray scattering studies of the size, shape, and hydration of catalase, Biochim. Biophys. Acta 26 (1957) 233–240.

[44] P. Chacón, J.F. Díaz, F. Morán, J.M. Andreu, Reconstruction of protein form with X-ray solution scattering and a genetic algorithm, J. Mol. Biol. 299 (2000) 1289–1302.

[45] J.B. Sumner, N. Gralén, The molecular weight of crystalline catalase, J. Biol. Chem. 125 (1938) 33–36.

[46] C. Tanford, R. Lovrien, Dissociation of catalase into subunits, J. Am. Chem. Soc. 84 (1962) 1892–1896.

[47] J.B. Sumner, A.L. Dounce, V.L. Frampton, Catalase, III, J. Biol. Chem. 136 (1940) 343–356.

[48] T.F. Kumosinski, H. Pessen, Estimation of sedimentation coefficients of globular proteins: an application of small-angle X-ray scattering, Arch. Biochem. Biophys. 219 (1982) 89–100.

[49] H. Durchschlag, P. Zipper, Calculation of hydrodynamic parameters of biopolymers from scattering data using whole-body approaches, Progr. Colloid Polym. Sci. 107 (1997) 43–57.

[50] H. Eisenberg, Forward scattering of light, X-rays and neutrons, Q. Rev. Biophys. 14 (1981) 141–172.

[51] O. Glatter, O. Kratky (Eds.), Small Angle X-Ray Scattering, Academic Press, London, 1982.

[52] H. Durchschlag, Small-angle X-ray scattering of proteins in relation to food systems, with special emphasis on enzymes and storage proteins, in: I.C. Baianu, H. Pessen, T.F. Kumosinski (Eds.), Physical Chemistry of Food Processes Vol. 2: Advanced Techniques, Structures, and Applications, Van Nostrand Reinhold, New York, 1993, pp. 18–117.

[53] S.E. Harding, On the hydrodynamic analysis of macromolecular conformation, Biophys. Chem. 55 (1995) 69–93.

[54] S.E. Harding, The intrinsic viscosity of biological macromolecules. Progress in measurement, interpretation and application to structure in dilute solution, Progr. Biophys. Molec. Biol. 68 (1997) 207–262.

[55] I.D. Kuntz, Hydration of macromolecules. III. Hydration of polypeptides, J. Am. Chem. Soc. 93 (1971) 514–516.

[56] T.F. Kumosinski, H. Pessen, Structural interpretation of hydrodynamic measurements of proteins in solution through correlations with X-ray data, Methods Enzymol. 117 (1985) 154–182.

[57] H. Pessen, T.F. Kumosinski, Parameter predictions from correlations between hydrodynamic and X-ray data in: I.C. Baianu, H. Pessen, T.F. Kumosinski (Eds.), Physical Chemistry of Food Processes, Vol. 2: Advanced Techniques, Structures, and Applications, Van Nostrand Reinhold, New York, 1993, pp. 274–306.

[58] H. Durchschlag, P. Zipper, Prediction of hydrodynamic parameters of biopolymers from small-angle scattering data, J. Appl. Cryst. 30 (1997) 1112–1124.

[59] B. Spotorno, L. Piccinini, G. Tassara et al., BEAMS (BEAds Modelling System): a set of computer programs for the generation, the visualization and the computation of the hydrodynamic and conformational properties of bead models of proteins, Eur. Biophys. J. 25 (1997) 373–384 and erratum 26 (1997) 417.

[60] B. Carrasco, J. García de la Torre, O. Byron et al., Novel size-independent modeling of the dilute solution conformation of the immunoglobulin IgG Fab' domain using SOLPRO and ELLIPS, Biophys. J. 77 (1999) 2902–2910.

[61] P. Zipper, H. Durchschlag, Prediction of hydrodynamic parameters of *Lumbricus terrestris* hemoglobin from small-angle X-ray and electron microscopic structures, Progr. Colloid Polym. Sci. (2001) in press.

[62] J. García de la Torre, S. Navarro, M.C. López Martínez, F.G. Díaz, J.J. López Cascales, HYDRO: A computer program for the prediction of hydrodynamic properties of macromolecules, Biophys. J. 67 (1994) 530–531.

[63] B. Carrasco, J. García de la Torre, P. Zipper, Calculation of hydrodynamic properties of macromolecular bead models with overlapping spheres, Eur. Biophys. J. 28 (1999) 510–515.

[64] P. Zipper, H. Durchschlag, Prediction of hydrodynamic parameters from 3D structures, Progr. Colloid Polym. Sci. 113 (1999) 106–113.

[65] J.L. Sussman, D. Lin, J. Jiang et al., Protein data bank (PDB): database of three-dimensional structural information of biological macromolecules, Acta Cryst. D54 (1998) 1078–1084.

[66] B. Lee, F.M. Richards, The interpretation of protein structures: estimation of static accessibility, J. Mol. Biol. 55 (1971) 379–400.

[67] F.M. Richards, The interpretation of protein structures: total volume, group volume distributions and packing density, J. Mol. Biol. 82 (1974) 1–14.

[68] F.M. Richards, Areas, volumes, packing, and protein structures, Annu. Rev. Biophys. Bioeng. 6 (1977) 151–176.

[69] F.M. Richards, Calculation of molecular volumes and areas for structures of known geometry, Methods Enzymol. 115 (1985) 440–464.

[70] M.L. Connolly, Solvent-accessible surfaces of proteins and nucleic acids, Science 221 (1983) 709–713.

[71] M.L. Connolly, Computation of molecular volume, J. Am. Chem. Soc. 107 (1985) 1118–1124.

[72] M.L. Connolly, The molecular surface package, J. Mol. Graph. 11 (1993) 139–141.

[73] Y.N. Vorobjev, J. Hermans, SIMS: Computation of a smooth invariant molecular surface, Biophys. J. 73 (1997) 722–732.

[74] H. Durchschlag, P. Zipper, G. Purr, R. Jaenicke, Comparative studies of structural properties and conformational changes of proteins by analytical ultracentrifugation and other techniques, Colloid Polym. Sci. 274 (1996) 117–137.

[75] H. Durchschlag, P. Zipper, R. Wilfing, G. Purr, Detection of small conformational changes of proteins by small-angle scattering, J. Appl. Cryst. 24 (1991) 822–831.

[76] H. Durchschlag, P. Zipper. Modeling of protein hydration with respect to X-ray scattering and hydrodynamics. Progr. Colloid Polym. Sci. (2001) in press.

[77] S.J. Perkins, Protein volumes and hydration effects, Eur. J. Biochem. 157 (1986) 169–180.

[78] S.J. Perkins, A.W. Ashton, M.K. Boehm, D. Chamberlain, Molecular structures from low angle X-ray and neutron scattering studies, Int. J. Biol. Macromol. 22 (1998) 1–16.

[79] C. Ebel, H. Eisenberg, R. Ghirlando, Probing protein–sugar interactions, Biophys. J. 78 (2000) 385–393.

[80] J.G. Grossmann, Z.H.L. Abraham, E.T. Adman et al., X-ray scattering using synchrotron radiation shows nitrite reductase from *Achromobacter xylosoxidans* to be a trimer in solution, Biochemistry 32 (1993) 7360–7366.

[81] H.-X. Zhou, Calculation of translational friction and intrinsic viscosity. II. Application to globular proteins, Biophys. J. 69 (1995) 2298–2303.

[82] B. Carrasco, J. García de la Torre, Hydrodynamic properties of rigid particles: comparison of different modeling and computational procedures, Biophys. J. 75 (1999) 3044–3057.

[83] J. García de la Torre, B. Carrasco, Intrinsic viscosity and rotational diffusion of bead models for rigid macromolecules and bioparticles, Eur. Biophys. J. 27 (1998) 549–557.

[84] H.B. Bull, Protein hydration: a sucrose probe, Arch. Biochem. Biophys. 208 (1981) 229–232.

[85] H. Eisenberg, Analytical ultracentrifugation in a Gibbsian perspective, Biophys. Chem. 88 (2000) 1–9.

[86] P. Chacón, F. Morán, J.F. Díaz, E. Pantos, J.M. Andreu, Low-resolution structures of proteins in solution retrieved from X-ray scattering with a genetic algorithm, Biophys. J. 74 (1998) 2760–2775.

[87] F. Bonneté, C. Ebel, G. Zaccai, H. Eisenberg, Biophysical study of halophilic malate dehydrogenase in solution: revised subunit structure and solvent interactions of native and recombinant enzyme, J. Chem. Soc. Faraday Trans. 89 (1993) 2659–2666.

[88] S.E. Harding, Modelling the gross conformation of assemblies using hydrodynamics: the whole body approach, in: S.E. Harding, A.J. Rowe (Eds.), Dynamic Properties of Biomolecular Assemblies, Royal Society of Chemistry, Cambridge UK, 1989, pp. 32–56.

[89] J.L. Oncley, Evidence from physical chemistry regarding the size and shape of protein molecules from ultracentrifugation, diffusion, viscosity, dielectric dispersion, and double refraction of flow, Ann. N.Y. Acad. Sci. 41 (1941) 121–150.

[90] I.D. Kuntz Jr., T.S. Brassfield, G.D. Law, G.V. Purcell, Hydration of macromolecules, Science 163 (1969) 1329–1331.

[91] S.E. Harding, A.J. Rowe, J.M. Creeth, Further evidence for a flexible and highly expanded spheroidal model for mucus glycoproteins in solution, Biochem. J. 209 (1983) 893–896.

[92] S.J. Perkins, K.F. Smith, J.M. Kilpatrick, J.E. Volanakis, R.B. Sim, Modelling of the serine-proteinase fold by X-ray and neutron scattering and sedimentation analyses: occurrence of the fold in factor D of the complement system, Biochem. J. 295 (1993) 87–99.

[93] K.A. Andrewartha, R.T.C. Brownlee, D.R. Phillips, Arch. Biochem. Biophys. 185 (1978) 423–428.

[94] A. Bairoch, R. Apweiler, The SWISS-PROT protein sequence database and its supplement TrEMBL in 2000, Nucleic Acids Res. 28 (2000) 45–48.

[95] J.C. Lee, S.N. Timasheff, Partial specific volumes and interactions with solvent components of proteins in guanidine hydrochloride, Biochemistry 13 (1974) 257–265.

[96] R.A. Sayle, E.J. Milner-White, Rasmol — biomolecular graphics for all, Trends Biochem. Sci. 20 (1995) 374–376.